Roto–translational motion in liquid water and its structural implication

I.M. Svishchev and P.G. Kusalik

Department of Chemistry, Dalhousie University, Halifax, Nova Scotia, Canada B3H 4J3

Received 10 September 1993; in final form 19 October 1993

The two nonvanishing cross-correlation functions between component of the linear and angular velocities for SPC/E water have been determined. We have used them to analyze the dynamics of coupled rotational translational motions in this liquid and have examined how this motion is manifest in its local structure. The dominant low-frequency modes in the power spectra of these cross-correlation functions are found to correspond well with the positions of peaks in the experimental Raman and infrared spectra of water.

1. Introduction

In recent simulation studies we have obtained the spatial distribution functions (SDF), $g_{OO}(r, \underline{\Omega})$ and $g_{OH}(r, \underline{\Omega})$, for SPC/E water and applied them to the analysis of the local equilibrium structure in this liquid [1]. One of these functions $g_{OO}(r, \underline{\Omega})$, proved particularly helpful in characterizing a nontetrahedral (interstitial) coordination in water. This SDF clearly displayed a local oxygen pair-density maximum at interstitial separations of about 3.5 Å which appeared confined to a relatively small range of orientations, $\underline{\Omega}$, in a local frame. Unfortunately, this maximum is lost in the angle-averaged radial distribution function (RDF) for liquid water [2], $g_{OO}(r)$, giving only an elevated pair density in the region of its first minimum. (In past, numerous attempts to identify this interstitial maximum from available diffraction data for $g_{OO}(r)$ has frequently lead to conflicting speculations on water structure [3].) Meanwhile, the dynamical implications of this interstitial coordination have remained largely unexplored. In this Letter we focus our attention on coupled rotational–translational motions of particles in liquid SPC/E water which appear to have direct consequences in the local structure, particularly the interstitial fraction.

In order to provide further motivation a full three-dimensional local density map for oxygen atoms in SPC/E water at 100°C is shown in fig. 1a, where we have plotted the isosurfaces corresponding to $g_{OO}(r, \underline{\Omega}) = 1.35$. In this figure we have denoted the first tetrahedrally coordinated neighbors as 1 and the additional coordination, which is confined to the upper hemisphere of the principal frame, as A. We see in fig. 1a that the oxygen density due to H-bond accepting neighbors appears as two well-defined caps positioned directly over the hydrogens of the central molecule, whereas only as single (banana-like) feature representing the density due to hydrogen (H-) bond donating nearest neighbors is observed. Qualitatively similar structures were noted in ref. [1] at lower temperatures. Yet perhaps the most striking feature in fig. 1a is the bridging of the oxygen density between the H-bond donating nearest neighbors and the neighbors corresponding to additional nontetrahedral coordination, denoted by A. One possible interpretation of this structural bridge is that it represents the minimum energy path on the average free energy surface (clearly, $g_{OO}(r, \underline{\Omega})$ could be expressed as a potential of mean force, $w_{OO}(r, \underline{\Omega})$) for a water molecule moving in the average local structure of the liquid. From a more dynamical standpoint, this path can be seen as a primary mechanism for the local diffusion of nearest neighbors in SPC/E water; hence it would also represent a principal means by which hydrogen bonds are broken (or made). From steric and kinematic considerations,

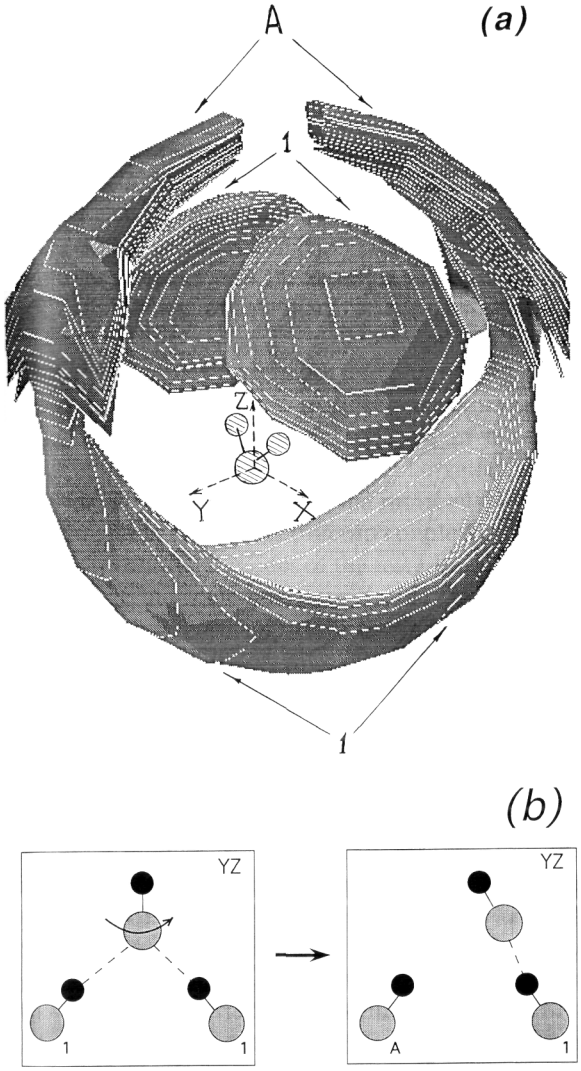

Fig. 1. (a) The oxygen–oxygen spatial distribution function presented as a three-dimensional map of the local oxygen density in liquid SPC/E water at 100°C. The iso-surface for $g_{OO}(r, \underline{\Omega}) = 1.35$ is shown. The central molecule has been included to define the local frame. 1 and A, respectively, identify the first tetrahedrally H-bonded neighbors and the additional nontetrahedral coordination. (b) A schematic representation as projected onto the YZ molecular plane of a coupled rotational–translational motion consistent with the bridged structure in (a).

we would predict that the motion responsible can be schematically depicted as in fig. 1b. The motion is characterized by the out-of-plane translational motion of a molecule accompanied by (or coupled with) the restricted rotation of its dipole vector about its x axis. As can be seen from fig. 1b, this coupled rotational translational motion of the central molecule can result in the displacement of a H-bond donating nearest neighbor to a more distant interstitial position (as viewed in the local frame of the central particle). The resulting arrangement is consistent with possible orientations of the interstitial neighbors identified in ref. [1].

The main purpose of the present study is then to test this hypothesis that specific translational and rotational motions can couple together to give rise to nontetrahedral coordination geometry in local water structure (as identified from $g_{OO}(r, \underline{\Omega}$ and $g_{OH}(r, \underline{\Omega})$). We do this by calculating those cross-correlation functions of the linear and angular velocities allowed by symmetry in SPC/E water. We have then analyzed their power spectra to determine how this motion may be manifest spectroscopically.

2. Simulation details

In this study we have used molecular dynamics (MD) simulations to examine the SPC/E model for liquid water [4]. Our simulation methodology have been discussed in detail in previous work [1,5] and hence only a few important points are given here. We define the local frame such that the dipole axis of the H_2O molecule lies along the Z axis and the molecular plane is in the XZ plane. Our simulation runs have been carried out with samples of 256 molecules at experimental densities 0.9981 g cm^{-3} and 0.9584 g cm^{-3}, respectively, and at constant temperatures of −10 and 100°C, controlled by means of a Gaussian thermostat [6]. The systems were equilibrated for about 100 ps at each temperature and the averages were collected over subsequent 250 ps trajectories. The Ewald summation technique has been employed to calculate the long-range interactions [7].

We have focused on two cross-correlation functions (CCF),

$$C_{xy}(t) = \frac{\langle v_x(t)\omega_y(0)\rangle}{\sqrt{\langle v_x^2\rangle\langle\omega_y^2\rangle}} = \frac{\langle v_x(0)\omega_y(t)\rangle}{\sqrt{\langle v_x^2\rangle\langle\omega_y^2\rangle}} \qquad (1)$$

and

$$C_{yx}(t)=\frac{\langle v_y(t)\omega_x(0)\rangle}{\sqrt{\langle v_y^2\rangle\langle\omega_x^2\rangle}}=\frac{\langle v_y(0)\omega_x(t)\rangle}{\sqrt{\langle v_y^2\rangle\langle\omega_x^2\rangle}}, \qquad (2)$$

which are the only nonvanishing functions for a system of particles of C_{2v} symmetry [8]. In eqs. (1) and (2), $\omega_\alpha(t)$ is the α component of the angular velocity at time t and $v_\alpha(t)$ is the α component of the linear velocity at time t resolved in the local frame at $t=0$. The large arrays spanning 8 ps used to store these CCFs during our runs have enabled us to determine their power spectra with relatively high resolution. The statistical errors in our cross-correlation functions have been estimated to be 4% using the procedure outlined by Allen and Tildesley [7]. These estimates were confirmed by monitoring the numerical noise in the vanishing (by symmetry) CCFs.

3. Results and discussion

The normalized cross-correlation functions $C_{xy}(t)$ and $C_{yx}(t)$ for SPC/E water at -10 and $100\,^\circ$C are shown in fig. 2. In general, our CCFs are qualitatively similar to those obtained in earlier work with other asymmetric tops [8,9]. Perhaps the most striking features of fig. 2a are the trough and the peak pair occurring in $C_{xy}(t)$ at about 0.4 and 0.7 ps, respectively. At $-10\,^\circ$C additional oscillations are also apparent (a more complete discussion of the temperature dependence is given below). This feature strongly suggests a resonant motion in the plane of a molecule, anchored by the H-bonds it forms with its H-bond donating neighbors, in which it simply rocks forward and then rocks back. Hence, we would expect no net motion due to the mode which is consistent with the two distinct structural features (caps) in $g_{OO}(r, \underline{\Omega})$ in the XZ plane due to H-bond accepting nearest neighbors (see fig. 1a). Examining fig. 2b, we find that $C_{yx}(t)$ exhibits distinctly different behavior; it is dominated by a single large positive peak at about 0.25 ps (followed by several smaller oscillations), suggestive of net motion. This motion can be characterized as one in which a molecule, anchored essentially at its hydrogens, rocks forward. Obviously, this is the same motion schematically represented in fig. 1b which was used to explain the bridging structure observed in fig. 1a. It is also important to point out the difference in scales

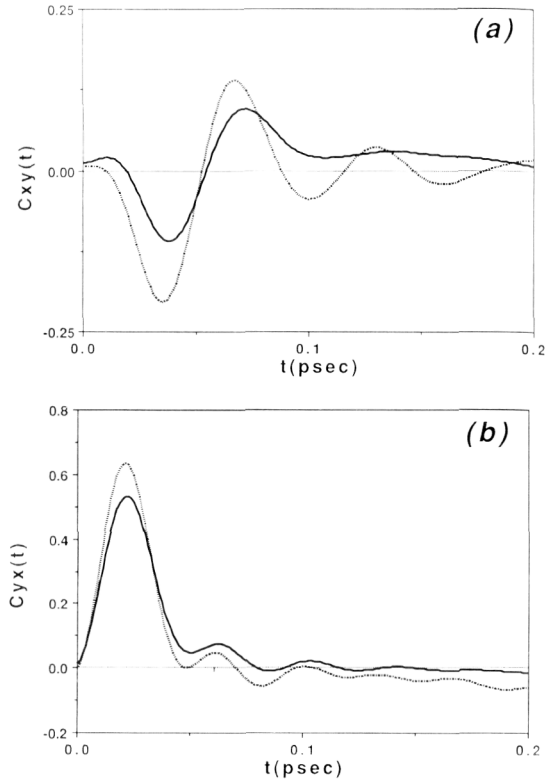

Fig. 2. Nonvanishing cross-correlation functions for SPC/E water at (——) $100\,^\circ$C and (– – –) $-10\,^\circ$C. (a) $C_{xy}(t)$ and (b) $C_{yx}(t)$.

used in fig. 2, indicating a much stronger coupling between v_y and ω_x than between v_x and ω_y.

Much of the quantitative difference between -10 and $100\,^\circ$C results in fig. 2 can be accounted for by the dependence of $C_{xy}(t)$ and $C_{yx}(t)$ upon the temperature (through the mean-square velocities appearing in eqs. (1) and (2)). Yet the consistently larger features in these normalized CCFs at $-10\,^\circ$C indicate a greater degree of coupling. In general, we find that the CCFs from $-10\,^\circ$C also exhibit stronger oscillatory behavior. Examining $C_{xy}(t)$ in fig. 2b we observe that the $-10\,^\circ$C result becomes obviously negative more quickly (this being a far less conspicuous feature at $100\,^\circ$C) suggesting the earlier (and stronger) onset of a rebound (or restoring) motion at lower temperatures. This is again consistent with our structural data; the bridge evident in fig. 1a at $100\,^\circ$C appears only at a much lower threshold, and

hence is a much more subtle feature at $-10°C$.

The power spectra of $C_{xy}(t)$ and $C_{yx}(t)$ at $-10°C$ are shown in fig. 3. These spectra contain considerable structure, and we will consider each separately. Focusing first on the spectrum of $C_{xy}(t)$ in fig. 3, which reflects the coupling between rotations and translations in the molecular plane, several modes can be identified. In addition to a high-frequency peak at about 500 cm^{-1}, it contains two low-frequency modes with the maxima at about 60 and 190 cm^{-1}. We recall that the latter two peaks can also be observed in the power spectrum of the X component of the auto-correlation function (ACF) of the linear velocity, while the high-frequency 500 cm^{-1} mode is a major (librational) feature of the spectrum of the Y component of the angular velocity ACF [5,10]. Clearly, the translational motion of the center-of-mass in the X direction can couple to either of two slow rotational modes of the fast librational motion of the molecule about its Y axis. However, we have already argued that this motion appears to result in no net displacement of the molecule.

From fig. 3 we see that the spectrum of $C_{yx}(t)$ contains one sharp maximum at low frequency centered at about 60 cm^{-1} and a broader minimum located at about 770 cm^{-1}. These features are apparently a result of interaction between the high-frequency librational mode observed at 750–780 cm^{-1} in the power spectrum of the X component of the angular velocity ACF and the major low-frequency translational mode (usually referred to as OOO bending mode of three H-bonded molecules [5,10,11]). This coupling is such that it can give rise to a net displacement, as represented in fig. 1b.

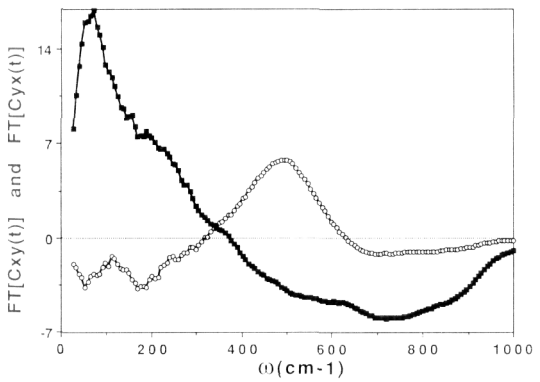

Fig. 3. Power spectra of cross-correlation functions (○) $C_{xy}(t)$ and (■) $C_{yx}(t)$ at $-10°C$.

We conclude this discussion by recalling that in our recent simulation study of the modes in the (allowed) infrared and Raman spectra for SPC/E water a roto–translational mode arising from the single-dipole orientational ACF [5] was clearly evident at 60 cm^{-1}. At the same time we were unable to find any evidence of a 190 cm^{-1} peak in the power spectrum of this ACF. This mode is well-documented in experimental optical spectra [11,12]. The present study focusing upon the cross-correlation functions for the SPC/E model has provided us with perhaps further insights into the low-frequency region. Fig. 3 suggests that the 190 cm^{-1} mode may, in fact, exist in the allowed optical spectra for this model; it has simply remained undetected because of its very low intensity.

4. Conclusions

In this Letter, we have reported results from MD simulations of liquid SPC/E water at -10 and $100°C$. We have determined $\langle v_x(t)\omega_y(0)\rangle$ and $\langle v_y(t)\omega_x(0)\rangle$, the only two nonvanishing cross-correlation functions between the linear and angular velocities for molecules of C_{2v} symmetry. We have used these CCFs to characterize the dynamics of coupled roto–translational motions in liquid water and have demonstrated how this motion is reflected in its average local structure. In particular, we have argued that an out-of-plane translation of a molecule coupled with a rotation about its X axis represents a mechanism by which a nearest H-bonded neighbor can be displaced (in the local frame) into an interstitial position, thereby providing an opportunity of local diffusion. The power spectra of the CCFs has also been calculated, examination of which reveals peaks at about 500 and 750 cm^{-1} (due to coupling with librational motions) and a peak at ≈ 60 cm^{-1} arising from low-frequency translational modes. The spectrum of $\langle v_x(t)\omega_y(0)\rangle$ also exhibits a weak roto–translational mode at about 190 cm^{-1}, which was previously thought to be absent in nonpolarizable models for water.

Acknowledgement

We are grateful for the financial support of the Natural Sciences and Engineering Research Council of Canada.

References

[1] I.M. Svishchev and P.G. Kusalik, J. Chem. Phys. 99 (1993) 3049.
[2] A.K. Soper and M.G. Phillips, Chem. Phys. 107 (1986) 47.
[3] D. Eisenberg and W. Kauzmann, The structure and properties of water (Oxford Univ. Press, 1969).
[4] H.J.C. Berendsen, J.R. Grigera and T.P. Straatsma, J. Phys. Chem. 91 (1987) 6269.
[5] I.M. Svishchev and P.G. Kusalik, J. Chem. Phys., submitted for publication.
[6] D.J. Evans and J.P. Morriss, Statistical mechanics of nonequilibrium liquids (Academic Press, New York, 1990).
[7] M.P. Allen and D.J. Tildesley, Computer simulations of liquids (Oxford Univ. Press, Oxford, 1987).
[8] M.W. Evans, J. Chem. Phys. 78 (1983) 926.
[9] M.W. Evans, G.C. Lie and E. Clementi, J. Chem. Phys. 87 (1987) 6040.
[10] R.W. Impey, P.A. Madden and I.R. McDonald, Mol. Phys. 46 (1982) 513.
[11] G.E. Walrafen, J. Chem. Phys. 40 (1964) 3249.
[12] K. Mizoguchi, Y. Hori and Y. Tominaga, J. Chem. Phys. 97 (1992) 1961.